A Non-Parametric Inference Technique for Shape Boundaries in Noisy Point Clouds

Selim Özgen, Florian Faion, Antonio Zea and Uwe D. Hanebeck[1]

***Abstract*— This study explores the non-parametric estimation of a shape boundary from noisy points in 2D when the sensor characteristics are known. As the underlying shape information is not known, the offered algorithm estimates points on the shape boundary by using the statistics of the subsets of point cloud data.**

The novel approach proposed in this paper is able to find corner points in a local geometry by only using sample mean and covariance matrices of the subsets of the point cloud. While the proposed approach can be used for any class of boundary functions that demonstrates symmetry; for this paper, the analysis and experiments are performed on a connected line segment.

I. Introduction

The last two and a half decades have witnessed a breakthrough both in the computational capacity and the sensor technologies. This comes with a trade-off; while it is possible to do burdensome calculations in a very little amount of time, using every bit of data would still bring a computational complexity and would be redundant considering the needs of the user. Therefore, getting rid of redundancy is a major challenge and it is affordable to downsample the sensor data as much as possible, if the quality of estimation is not decreasing with the downsampling. Consider the environment perception problem with laser scanners; if the aim is to discriminate between curved and flat surfaces immediately, the noisy point cloud measured by the laser scanner would be highly redundant and can be downsampled with some basic statistical tests.

In this paper, we deal with extended objects, where an object causes multiple measurements in each observation. These measurements are assumed to be generated from multiple point sources on the boundary of the object. For simplicity, the boundary function is assumed to be a hypersurface, but the parametric form of this hypersurface is unknown. While the measurement sources lie on a hypersurface, the measurements are *noisy*, so that there is no guarantee that they lie on the boundary of the target shape.

If the user has an idea about the underlying shape, the reasonable idea would be to explicitly model the shape with a set of state parameters. Any instant of these state parameters would mean another realization of the shape function. The usual approach to estimate the "best" shape parameters is to associate each measurement in some way to the sources on the shape, which allows for the derivation of a value or metric to be minimized or maximized. Finding the set of shape parameters that fit best to a list of given point measurements is called *shape fitting*. There is a field of research mainly in computer vision that deals with fundamental geometries such as conics [1], [2], rectangles [3], and line segments [3].

Yet, the selection of an underlying shape function is only a part of the problem while there is also an uncertainty about the actual measurement source that has caused the measurement. This uncertainty about the actual measurement source is called the *association problem*. For this problem, viable approaches can be classified into two categories; that consider multiple sources probabilistically [3], [4], and approaches that consider only a single best-fitting source [5], [6] which minimizes some metric. When only a single measurement source from the shape boundary is to be selected, a common approach is to minimize the sum of square Euclidean distances between measurements and their closest points [5], [7], also denoted as *least squares* approaches. As these techniques do not require a probabilistic modeling, they have the advantage of easier implementation. Yet, as these approaches do not consider the properties of the shape function, they have a problem of estimation bias [2], [8] when the selected measurement source resides in a highly nonlinear part of the shape.

Taking multiple measurement sources into consideration comes with a computational burden, but results in a robust estimator. Werman and Keren [3] have shown this by considering each point on the model as a measurement source for each individual measurement. As every measurement source is taken into account for each measurement, their model is called Spatial Distribution Model. Recently, Partial Information Models [8] were proposed to tackle the same problem. These models also find the closest point from the measurement to the shape function but then consider the *partial likelihood* [9] for this given measurement source. Both approaches result in an unbiased estimator even when the underlying shape function has a high curvature or strong discontinuities.

Assume that you are given sparse point measurements with a known noise model originating from a shape boundary. If the underlying shape function is *not parametrized*, how much can we infer about the shape information? This depends on two conditions. First, there must be "sufficient" number of measurements coming from the extended object. This is reasonable, as with a small number of measurements, the statistical inference would also be weak. Second, the sensor properties must be well known, as the shape function is assumed to be unknown. Without a good statistical knowledge about the sensor, the estimator would not be robust.

Werman and Keren [3] have extended their Spatial Distribution Model for non-parametric curves. For this, they

[1]The authors are with the Chair of Intelligent Sensor-Actuator-Systems (ISAS) at the Karlsruhe Institute of Technology (KIT), Germany. selim.oezgen@kit.edu, florian.faion@kit.edu, antonio.zea@kit.edu, uwe.hanebeck@ieee.org

take a set of discrete points as the shape function and use a global objective function that minimizes the distance of measurements to all of these discrete points. However, the question of how to select these discrete points and how to change their location for increasing and decreasing local curvatures on the boundary function is still not answered and shows the necessity of parameterization. They also discussed another problem of a purely Bayesian approach for non-parametric curve fitting: it is possible that a non-parametric shape function would "curl around" the data point to increase the likelihood of receiving this data point.

Instead of assigning a set of discrete points as the shape function, our aim is to arrive at these points by using some simple statistical techniques. A simple estimator would be taking the subsets of the data points according to a procedure and assuming that the mean of these points are on the shape boundary. There is a vastly used procedure in computer vision called mean shift for finding the modes of a density function. Mean shift algorithm uses a certain rule on the subsets of given data points to find the mode in an iterative manner. This rule is known as the kernel function.

Yet, the mode detected by the mean shift algorithm is not necessarily on the shape boundary. This is called the estimation bias. There is a line of work showing that, for a given parametric model, the bias of the estimation is directly related to the curvature of hypersurface [2], [10], [11] and this idea can be extended to the local geometries when the curvature is infinite [12]. This approach is not directly applicable to non-parametric estimation. But the idea can be extended to explain the results of the statistical tests we are offering.

This paper uses simple statistical tools such as the sample mean and covariance matrix for the estimation of the bias when the curvature of the local geometry is high. By using these statistical tools, we would alleviate the bias problem and arrive at a discrete number of points which we assume to be on the shape boundary. This is actually a downsampling technique that can be useful when the shape boundary is a complex function and therefore, calculating the likelihood for each measurement would be computationally costly.

II. Problem Formulation

In mathematical terms, assume that the boundary of the target shape is a set of uncountably infinite points $\mathcal{S}_x$, which we assume is a hypersurface and can be parametrized by a state vector $\underline{x}$ not known by the user. We want to gain information about $\mathcal{S}_x$ from the point measurements $\mathcal{Y} = \{\underline{y}_1, \cdots, \underline{y}_m\}$ given in Cartesian coordinates.

Each measurement $\underline{y}_i$ is generated by the following stochastic measurement model: a measurement source $\underline{z}_i \in \mathcal{S}_x$ is selected from the shape boundary. Then, this source is corrupted by an additive noise term $\underline{v}_i$, which is Gaussian distributed;

$$\underline{y}_i = \underline{z}_i + \underline{v}_i, \quad \underline{v}_i \sim \mathcal{N}(\underline{0}, \mathbf{C}_v) \ , \tag{1}$$

yielding the measurement $\underline{y}_i$. In this study, we will focus on isotropic noise, i.e., $\mathbf{C}_v = \sigma^2 \cdot \mathbf{I}$, where σ^2 is a known term. Furthermore, we assume that the noise term $\underline{v}_i$ is independent from the state and $\underline{v}_i$ and $\underline{v}_j$, $i \neq j$ are uncorrelated.

Suppose that we are able to explicitly model the shape boundary $\mathcal{S}_x$ with the state vector $\underline{x}$ and have information about its *a priori* probability distribution $p(\underline{x})$. Then, the sparse point measurements $\mathcal{Y}$ can be used for updating our information about the state vector $\underline{x}$ by the aid of well known Bayes' rule

$$p(\underline{x} \,|\, \mathcal{Y}) \propto p(\mathcal{Y} \,|\, \underline{x}) p(\underline{x}) \ . \tag{2}$$

However, our problem here is not the uncertainty about the state vector $\underline{x}$. As the shape itself is unknown in advance, there is no reasonable model we can apply, and in consequence, no meaningful parameters to estimate.

Without a known model of the shape, our aim is to find points $\mathcal{Z} = \{\underline{z}_1, \cdots, \underline{z}_k\}$ on the shape boundary such that $\mathcal{Z} \subset \mathcal{S}_x$. While $\mathcal{S}_x$ is a set of uncountably infinite points that form the shape boundary, $\mathcal{Z}$ described here is a set of a finite number of points. Now define $\mathcal{S}_\mathcal{Z}$ as the function of the shape boundary which is formed by interpolating the points in the set $\mathcal{Z}$. If the set $\mathcal{Z}$ contains enough data points from the shape boundary especially where the curvature of the shape boundary is high, then $\mathcal{S}_\mathcal{Z} \approx \mathcal{S}_x$.

Then, for the non-parametrized case, we start with a set of measurement points $\mathcal{Y}$ and end up with a set of points $\mathcal{Z}$ which we assume to be on the shape boundary and $|\mathcal{Z}| \ll |\mathcal{Y}|$. We will infer this information from our knowledge about the sensor model and the statistical tests that we apply on subsets of the noisy point clouds. This can be compared to a maximum likelihood approach in which we are trying to find a set of measurement sources $\mathcal{Z}$ that would maximize the likelihood $p(\mathcal{Y} \,|\, \mathcal{Z})$. So, with a slight abuse of notation, the problem can be formulated as;

$$p(\mathcal{Z} \,|\, \mathcal{Y}) \propto p(\mathcal{Y} \,|\, \mathcal{Z}) p(\mathcal{Z}) \tag{3}$$

Note that this formulation is only for providing a better understanding of the approach and not usable because $\mathcal{Z}$ is not a predefined set with known properties. As the measurements can be treated individually, we will write

$$p(\mathcal{Y} \,|\, \mathcal{Z}) = \prod_{i=0}^{m} p(\underline{y}_i \,|\, \mathcal{Z}) \ , \tag{4}$$

In the following formulas, the subindex i will be dropped unless needed.

III. Properties of the Shape Function

We will start our discussion by describing the local geometry of $\mathcal{S}_x$ in mathematical terms. For the sake of simplicity, we will constrain ourselves with 2D for the rest of this paper. Let $\underline{z}_x(s)$, for $s \in [s_0, s_T] \subset \mathbb{R}$, be an arbitrary regular arc length parametrization of the shape boundary as shown in Fig. 1. That is, $\underline{z}_x(s)$ is differentiable except for a countable number of points, does not jump backwards, and between $\underline{z}_x(s_a)$ and $\underline{z}_x(s_b)$ it traverses an arc with length $s_b - s_a$. We can therefore denote s as the *source parameter*. It can be seen that $\underline{z}'_x(s)$ determines the tangent at the position

s. Analogously, we can define $\underline{n}_x(s)$ as the function which returns the normal at point s such that $\underline{z}'_x(s) \cdot \underline{n}_x(s) = 0$. We will further select $\|\underline{n}_x(s)\| = 1$ and $\|\underline{z}'_x(s)\| = 1$.

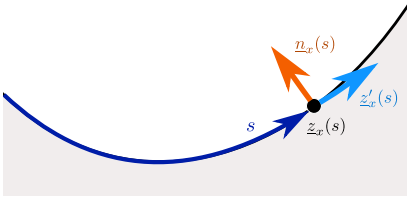

Fig. 1: Parametrization for the curve in black. For a given parameter s, the function $\underline{z}_x(s)$ selects the corresponding source. The tangent at this point is $\underline{z}'_x(s)$, and the normal is $\underline{n}_x(s)$ and points outwards. Grey is the shape interior.

Then, the generative model in (1) can be described in the following way. First, we randomly draw a parameter $s \in [s_0, s_T]$ according to a distribution $p(s \,|\, \underline{x})$. This yields the source $\underline{z}_x(s)$. Second, this source is corrupted by the Gaussian noise term $\underline{v}$ according to (1). From this, we obtain the measurement equation

$$\underline{y} = \underline{z}_x(s) + \underline{v} \tag{5}$$

Using $\underline{z}'_x(s)$ and $\underline{n}_x(s)$ as the basis vectors in 2D, we can write (5) as

$$\underline{y} = \underline{z}_x(s) + s_v \cdot \underline{z}'_x(s) + l_v \cdot \underline{n}_x(s) \tag{6}$$

where $s_v = \underline{v} \cdot \underline{z}'_x(s)$ and $l_v = \underline{v} \cdot \underline{n}_x(s)$. We can make an important observation here: It can be seen that l_v and s_v will be independent variables if (and only if) $\underline{z}'_x(s)$ and $\underline{n}_x(s)$ coincide with the *principal components* of the Gaussian measurement covariance matrix $\mathbf{C}_v$. Note that, with our assumption of isotropic measurement noise, this case is always satisfied.

The underlying shape function $\underline{z}_x(s)$ can be seen as a combination of infinite number of point sources. We now want to further our analysis for different shape functions starting from point sources.

A. $\underline{z}_x(s)$ as a Single Point Source

Assume that we have a point measurement source $\underline{z} = [a\ b]^T$ that resides in a sl coordinate system. For any given measurement $\underline{y}$, $l_v = l - b$ and $s_v = s - a$ describe the distance of the measurement from the point source $\underline{z}$. As the noise $\underline{v}$ is isotropic, we can write,

$$p(l_v, s_v) = p(l_v)p(s_v) \tag{7}$$

Now take the region $\mathcal{R}_z$ extending from $s = -A$ to $s = A$ as shown in Fig. 2. In accordance with the terminology of the mean shift algorithm, we will call $\mathcal{R}_z$ as a kernel. Note that,

$$p(l_v, s_v|\mathcal{R}_z) = p(l_v|\mathcal{R}_z)p(s_v|\mathcal{R}_z) \tag{8}$$

where $\mathcal{R}_z$ stands for the event $\underline{y} \in \mathcal{R}_z$. Moreover,

$$p(l_v|\mathcal{R}_z) = \mathcal{N}(l; b, \sigma^2) = \mathcal{N}(l_v; 0, \sigma^2) \tag{9}$$

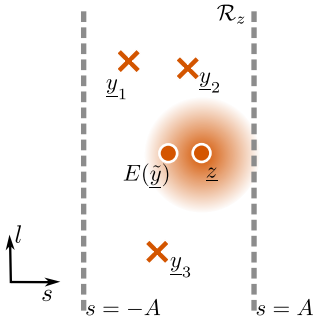

Fig. 2: A point measurement source $\underline{z}$ is inside the kernel $\mathcal{R}_z$. $\mathcal{R}_z$ extends from $s = -A$ to $s = A$. Graph shows three instants of the random variable $\tilde{\underline{y}} = \{\underline{y} : \underline{y} = \underline{z} + \underline{v}, \underline{y} \in \mathcal{R}_z\}$. $E(\tilde{\underline{y}})$ is the expected value of $\tilde{\underline{y}}$.

Similarly for the s dimension,

$$p(s_v|\mathcal{R}_z) = \begin{cases} C\mathcal{N}(s; a, \sigma^2) & \text{if } s \in [-A, A] \\ 0, & \text{otherwise} \end{cases} \tag{10}$$

$C = \frac{1}{p(\underline{y} \in \mathcal{R}_z)}$ is the normalization constant. Then,

$$\begin{aligned} p(\underline{y} \in \mathcal{R}_z) &= p(-A - a \leq s_v \leq A - a) \\ &= \frac{1}{2}\left(\text{erf}\left(\frac{A+a}{\sigma\sqrt{2}}\right) + \text{erf}\left(\frac{A-a}{\sigma\sqrt{2}}\right)\right) \end{aligned} \tag{11}$$

where $\text{erf}\,(.)$ is the error function. Notice that, the distribution of the measurements in the s dimension is dependent on the width of the kernel $\mathcal{R}_z$ and the position of the measurement source a. We can make the following observations,

$$E(s_v|\mathcal{R}_z) = \frac{1}{p(\underline{y} \in \mathcal{R}_z)} \int_{-A}^{A} s_v \mathcal{N}(s; a, \sigma^2) ds \tag{12}$$

$$var(s_v|\mathcal{R}_z) \leq \sigma^2 \tag{13}$$

while $var(s_v|\mathcal{R}_z)$ would be exactly equal to σ^2 if $\mathcal{R}_z$ would extend to infinity in the s dimension. Also if $a \neq 0$, then $E(s_v|\mathcal{R}_z) \neq 0$. Finally, $\text{cov}[l_v, s_v|\mathcal{R}_z] = 0$ as l_v and s_v are independent.

B. $\underline{z}_x(s)$ as Multiple Point Sources

Assume that there are two point measurement sources $\mathcal{S}_x = \{\underline{z}_i,\ i = 1, 2\}$. As there are more than one measurement sources now, it is not reasonable to use l_v and s_v which is used the show the distance of the measurement to the measurement source, but use the general coordinates of the measurements s and l. Define the random variables

$$\tilde{\underline{y}} \sim p(\underline{y}|\mathcal{R}_z)$$
$$\tilde{\underline{y}}_i \sim p(\underline{y}|\underline{z} = \underline{z}_i, \mathcal{R}_z)$$

Denote the mean and covariance of $\tilde{\underline{y}}_i$ with μ_i and $\mathbf{C}_i$ and $\tilde{\underline{y}}$ with μ and $\mathbf{C}$, respectively. From Section III-A, we know that $\mathbf{C}_i$ is a diagonal matrix. We can write $p(\underline{y}|\mathcal{R}_z)$ as a mixture density,

$$p(\underline{y}|\mathcal{R}_z) = \sum_i p(\underline{z} = \underline{z}_i|\mathcal{R}_z)p(\underline{y}|\underline{z} = \underline{z}_i, \mathcal{R}_z) \tag{14}$$

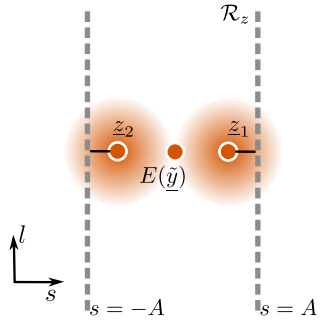

Fig. 3: Two point measurement sources $\underline{z}_1 = [a\ b]^T$ and $\underline{z}_2 = [-a\ b]^T$ inside kernel $\mathcal{R}_z$. $E(\underline{\tilde{y}})$ for the random variable $\underline{\tilde{y}} \sim p(\underline{y}|\mathcal{R}_z)$ is on the $s=0$ line.

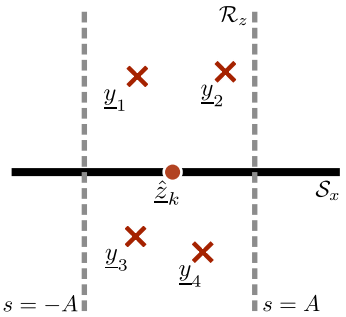

Fig. 4: All measurements $\mathcal{Y} = \{\underline{y}_1, \ldots, \underline{y}_4\}$ are originating from a linear boundary $\mathcal{S}_x$. The aim is to find an estimate $\underline{\hat{z}}_k \in \mathcal{S}_x$. For this, we just consider the measurements inside $\mathcal{R}_z$.

where $p_i = p(\underline{z} = \underline{z}_i|\mathcal{R}_z)$ is the mixing parameter and $\sum_i p_i = 1$. The first two moments of $p(\underline{y}|\mathcal{R}_z)$ would be calculated as follows;

$$\begin{aligned} \mu &= \sum_i p_i \mu_i \\ \mathbf{C} &= \sum_i p_i (\mathbf{C}_i + (\mu - \mu_i)(\mu - \mu_i)^T) \end{aligned} \tag{15}$$

We can see that if $\underline{z}_1 = [a\ b]^T$ and $\underline{z}_2 = [-a\ b]^T$, $\mu = [0\ b]^T$ and $\mathbf{C}$ would also be a diagonal matrix. Therefore $\mathrm{cov}[l, s|\mathcal{R}_z] = 0$. As shown in Fig. 3, when the underlying shape function $\underline{z}_x(s)$ preserves a symmetry around the $s=0$ axis, $\mathrm{var}(\underline{\tilde{y}})$ would be a diagonal matrix.

Moreover, (7) and (8) are still valid. As $p(\underline{z} = \underline{z}_1) = p(\underline{z} = \underline{z}_2)$ we can write $p_i \propto p(\underline{y} \in \mathcal{R}_z|\underline{z}_i)$. From (11), the mixing parameter becomes $p_i = 0.5$. Then,

$$p(l|\mathcal{R}_z) = \mathcal{N}(l; b, \sigma^2) \tag{16}$$

$$p(s|\mathcal{R}_z) = C(\mathcal{N}(s; a, \sigma^2) + \mathcal{N}(s; -a, \sigma^2)),\ s \in [-A, A] \tag{17}$$

where C is the normalization constant. Using (12),

$$E(s|\mathcal{R}_z) = 0 \tag{18}$$

C. $\underline{z}_x(s)$ as a Linear Function

Taking $\underline{n}_x(s) = [0\ 1]^T$ in (6), we arrive at $\mathcal{S}_x = \{[s\ b]^T |\ s \in [-s_T, s_T]\}$. For using the results of Section III-B define the set $\mathcal{S}_x(s) = \{\underline{z}_x(s), \underline{z}_x(-s)\}$. Then,

$$p(\underline{y}|\mathcal{R}_z) = \int_0^{s_T} p(\underline{y}|\underline{z} \in \mathcal{S}_x(s), \mathcal{R}_z) p(\underline{z} \in \mathcal{S}_x(s)|\mathcal{R}_z) ds \tag{19}$$

Note that the mixing parameter $p(\underline{z} \in \mathcal{S}_x(s)|\mathcal{R}_z)$ is different for each value of s. But from Section III-B, we know $E(\underline{y}|\underline{z} \in \mathcal{S}_x(s), \mathcal{R}_z) = [0\ b]^T,\ \forall s$. Therefore, we can write $E(\underline{y}|\mathcal{R}_z) = [0\ b]^T$. Added to that as $var(\underline{y}|\underline{z} \in \mathcal{S}_x(s), \mathcal{R}_z)$ is a diagonal matrix for all s, using (15) we can conclude that $\mathrm{cov}(\underline{y}|\mathcal{R}_z)$ is a diagonal matrix. For this selection of the boundary function, (7) and (8) are valid. Also,

$$p(l|\mathcal{R}_z) = \mathcal{N}(l; b, \sigma^2) \tag{20}$$

$$p(s|\mathcal{R}_z) = C \int_{-s_T}^{s_T} \mathcal{N}(s; s', \sigma^2) ds',\ s \in [-A, A] \tag{21}$$

D. $\underline{z}_x(s)$ as a Nonlinear Function

The idea described in Section III-B can be applied to all of the boundary functions that demonstrate symmetry around the $s=0$ axis. Certainly, the derivations for different boundary functions will differ from each other. For this paper, we two line segments connected at an end point. The demonstration of the problem is given in Fig. 5. The boundary function can be parameterized as $\underline{z}_x(s) = [s\ m|s|]^T,\ s \in [-s_T, s_T], m \in \mathbb{R}^+$. Define the arc length parameter as s'. Note that for any point on the shape boundary, $ds' = \sqrt{(ds^2 + dl^2)} = ds\sqrt{m^2+1}$.

Similar to Section III-C, we define the set $\mathcal{S}_x(s) = \{\underline{z}_x(s), \underline{z}_x(-s)\}$. For the s dimension, using (18) and (19), we can see $E(s|\mathcal{R}_z) = 0$. Again as $var(\underline{y}|\underline{z} \in \mathcal{S}_x(s), \mathcal{R}_z)$ is a diagonal matrix for all s, using (15) we can conclude that $\mathrm{cov}(\underline{y}|\mathcal{R}_z)$ is a diagonal matrix.

For the l dimension, we first calculate,

$$p(\underline{y} \in \mathcal{R}_z) = \int_{-s_T}^{s_T} p(\underline{y} \in \mathcal{R}_z|\underline{z} = \underline{z}_x(s)) p(\underline{z} = \underline{z}_x(s)) ds \tag{22}$$

$$= \frac{1}{2s_T} \int_0^{s_T} p(\underline{y} \in \mathcal{R}_z|\underline{z} = \underline{z}_x(s)) ds \tag{23}$$

$$= \frac{1}{s_T} \int_0^{s_T} \left(\mathrm{erf}\left(\frac{A+s}{\sigma\sqrt{2}}\right) + \mathrm{erf}\left(\frac{A-s}{\sigma\sqrt{2}}\right) \right) ds \tag{24}$$

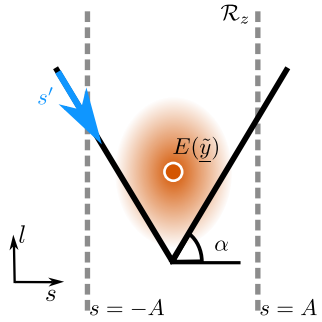

Fig. 5: $\mathcal{S}_x$ is a corner of a polygon parameterized as $\underline{z}_x(s) = [s\ m|s|]^T$ where $m = \tan(\alpha)$. $E(\underline{\tilde{y}})$ for the random variable $\underline{\tilde{y}} \sim p(\underline{y}|\mathcal{R}_z)$ is on the $s = 0$ line. Due to the symmetry in the shape function, $\text{cov}(\underline{\tilde{y}})$ is a diagonal matrix in the sl coordinates.

where we have used (11). Then,

$$E(l|\mathcal{R}_z) = \int_{-s_T}^{s_T} E(l|\underline{z} = \underline{z}_x(s), \mathcal{R}_z) p(\underline{z} = \underline{z}_x(s)|\mathcal{R}_z) ds \tag{25}$$

$$= \frac{m}{s_T} \int_0^{s_T} s \frac{p(\underline{y} \in \mathcal{R}_z|\underline{z} = \underline{z}_x(s)) p(\underline{z} = \underline{z}_x(s))}{p(\underline{y} \in \mathcal{R}_z)} ds \tag{26}$$

$$= \frac{m}{s_T C} \int_0^{s_T} s \left(\text{erf}\left(\frac{A+s}{\sigma\sqrt{2}}\right) + \text{erf}\left(\frac{A-s}{\sigma\sqrt{2}}\right)\right) ds \tag{27}$$

where $C = p(\underline{y} \in \mathcal{R}_z)$. Assuming $s_T \to \infty$,

$$E(l|\mathcal{R}_z) = \frac{m\sigma\sqrt{2}}{a} \left(\frac{(2a^2+1)\,\text{erf}\,(a)}{2} + \frac{a \exp(-a^2)}{\sqrt{\pi}} \right) \tag{28}$$

where $a = \frac{A}{\sigma\sqrt{2}}$. For the variance,

$$var(l|\mathcal{R}_z) = \sigma^2 + E(l^2|\mathcal{R}_z) - E(l|\mathcal{R}_z)^2 \tag{29}$$

$$E(l^2|\mathcal{R}_z) = m^2\sigma^2 \frac{2a^2+3}{3} \tag{30}$$

as can be seen when $m \to 0$, $var(l|\mathcal{R}_z) \to \sigma^2$ as expected.

IV. Shape Inference

In Section II, we have described the problem as finding discrete points $\underline{z}_k \in \mathcal{S}_x$. How can we use the statistical analysis of point sources for shape inference? Clearly, the set of points, $\mathcal{Z}$, that can be detected by statistical inference, is highly dependent on where they reside on the shape boundary $\mathcal{S}_x$.

First assume that we have a linear boundary function as shown in Fig. 4 and all measurements are i.i.d. Take all measurements $\mathcal{Y} = \{\underline{y}_i | \underline{y}_i \in \mathcal{R}_z\}$ and $N := |\mathcal{Y}|$. For the sample mean $\hat{\underline{z}} = \frac{\sum_{i=1}^N \underline{y}_i}{N}$,

$$E(\hat{\underline{z}}|\mathcal{R}_z) = E(\underline{y}|\mathcal{R}_z) = [0\ b]^T \tag{31}$$

$$\text{cov}(\hat{\underline{z}}|\mathcal{R}_z) = \text{cov}(\underline{y}|\mathcal{R}_z)/N \tag{32}$$

Therefore as N gets larger, $\hat{\underline{z}}$ approaches to $[0\ b]^T$. Define scalar variables $l_z = \underline{t} \cdot \hat{\underline{z}}$ and $s_z = \underline{n} \cdot \hat{\underline{z}}$. Note that l_z, which is the distance to the linear boundary, is an unbiased and consistent estimator.

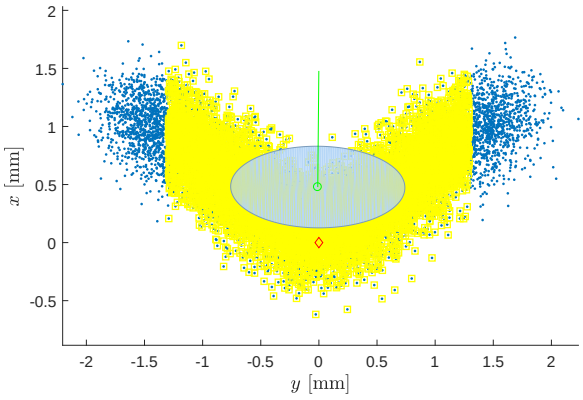

Fig. 6: For a given noisy point cloud, the mean shift algorithm is initiated using a circular kernel $\mathcal{C}_z$. The point where the mean shift algorithm stops is shown with a green circle. At this point, the sample covariance $\hat{\mathbf{C}}_z$ is calculated using the points inside $\mathcal{C}_z$. We switch to the kernel $\mathcal{R}_z$ by using the eigenvectors of $\hat{\mathbf{C}}_z$. The points in yellow squares shows the points inside $\mathcal{R}_z$. From these points, $\hat{\mathbf{C}}_z$ is calculated again. The eigenvector of $\hat{\mathbf{C}}_z$ that corresponds to $\hat{\sigma}_{l_z}$ is shown with a green line. Our aim is to find m and the corner point which is shown with a red diamond.

Up to this point, we have assumed that the kernel $\mathcal{R}_z$ is aligned with the sl axis and used this fact in our calculations. But we don't have prior knowledge of the shape boundary, and therefore, of s and l. This problem can be handled as follows; we will use a circular kernel $\mathcal{C}_z$ where the radius of the circle is a function of σ and calculate the sample covariance $\hat{\mathbf{C}}_z = \frac{\sum_{i=1}^N (\underline{y}_i - \hat{\underline{z}})(\underline{y}_i - \hat{\underline{z}})^T}{N-1}$. Singular value decomposition would give,

$$\hat{\mathbf{C}}_z = \mathbf{V}^T \hat{\mathbf{D}} \mathbf{V} \tag{33}$$

where $\mathbf{V} = [\underline{t}\,\underline{n}]$ and $\hat{\mathbf{D}} = diag(\hat{\sigma}^2_{l_z}, \hat{\sigma}^2_{s_z})$. Here, $\hat{\sigma}_{l_z}$ and $\hat{\sigma}_{s_z}$ are the sample standard deviations of l_z and s_z, respectively. But $\hat{\sigma}_{l_z}$ and $\hat{\sigma}_{s_z}$ are found by using $\mathcal{C}_z$ which would be a poor estimator. Vectors $\underline{t}$ and $\underline{n}$ can then be used for selection of the kernel $\mathcal{R}_z$ and $\hat{\mathbf{C}}_z$ is calculated again using $\mathcal{R}_z$. This process can be repeated until $\underline{t}$ and $\underline{n}$ converges to a value. This procedure holds in any of the cases in which the covariance matrix is diagonal. For a linear function, the sample covariance is an unbiased and consistent estimator $\hat{\sigma}_{l_z} \to \sigma$ with increasing sample size N. For a connected line segment, we have seen that $var(l|\mathcal{R}_z)$ increases with increasing m from (29). Therefore, the value of $\hat{\sigma}_{l_z}$ can be used as an identifier which shows if we are on a linear region of the shape function.

V. Evaluation

For the experimental setup, we assume that we have a noisy point cloud originating from a connected line segment. The experiments were repeated for α varying from $\pi/10$ to $4\pi/10$ radians and for different number of data points, N. In all experiments, the standard deviation of the isotropic noise σ_v is taken as 0.2mm while the length of each line segment is 2mm. Our aim is to find the corner point $\underline{z}_k$ and

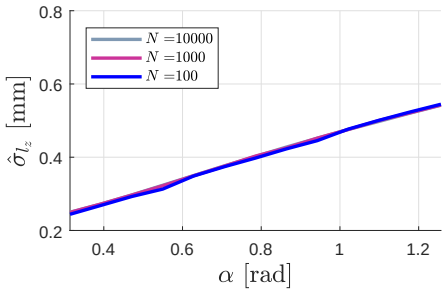

(a) The mean value for $\hat{\sigma}_{l_z}$

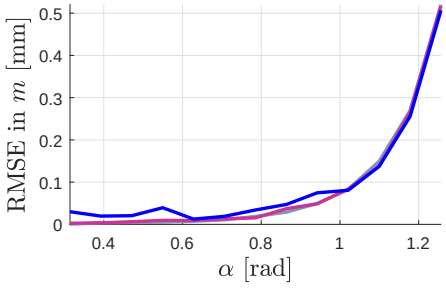

(b) Mean square error for m

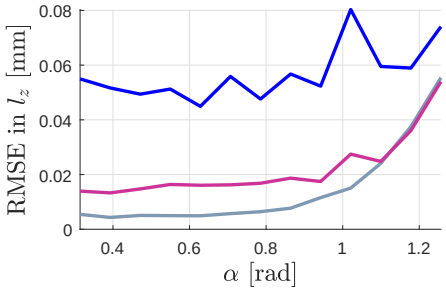

(c) Mean square error for l_z

Fig. 7: Results for 100 trials with different number of data points N. The measurement noise is isotropic with $\sigma = 0.2$mm.

estimate the angle between the line segments, or equivalently, the slope $m = \tan(\alpha)$. One instant of the experiments is shown in Fig. 6. The kernel width A is selected such that $A < s_T$.

The average results for 100 trials are shown in Fig. 7. Recall that the lower bound for $\hat{\sigma}_{l_z}$ is $\sigma = 0.2mm$ when $m = 0$. This is consistent with Fig. 7a where a general trend for $\hat{\sigma}_{l_z}$ can be observed in all results for N ranging from 10^2 to 10^4. However, the estimation of m and l_z are highly dependent on the value of $\hat{\sigma}_{l_z}$. Small differences in the estimator $\hat{\sigma}_{l_z}$ cause much difference in the estimation of m and l_z as can be seen from Fig. 7b and 7c, respectively. None of the estimators were able to alleviate the bias totally, but the best results were taken for small values of α when N is large. The estimation quality decreases when α is increased. This is an expected result; as the spread of the means term in (15) starts playing a larger role in the calculation of the sample covariance matrix $\hat{\mathbf{C}}_z$ for the selected kernel $\mathcal{R}_z$.

VI. Conclusions

In this paper, we have proposed an novel method for the non-parametric estimation of a shape boundary in a noisy point cloud. The subsets of the point cloud has been taken into account to find out the linear and non-linear parts of the shape boundary. While there is a literature on the parametric estimation methods of the problem, the non-parametric estimation problem is not much delved into due to its complexity.

There are a number of subjects with the proposed method that should be considered. First of all, the method is highly dependent on the number of samples as the sample covariance matrix is used in the estimation process. Moreover, the assumption that the noise statistics are perfectly known might be unrealistic. However, due to the simplicity of the method proposed, these problems can be afforded.

In this study, the analytical results for $E(l|\mathcal{R}_z)$ and $var(l|\mathcal{R}_z)$ were used in the estimation process. It is also possible to analytically calculate $var(s|\mathcal{R}_z)$ for different shape functions and incorporate this information into the estimation process. Also, the selection of another kernel function besides $\mathcal{R}_z$, where l dimension is also finite would be beneficial to decrease the error in the estimation of m and l_z for high values of α.

References

[1] M. Baum and U. D. Hanebeck, "Fitting Conics to Noisy Data Using Stochastic Linearization," in *Proceedings of the 2011 IEEE/RSJ International Conference on Intelligent Robots and Systems (IROS 2011)*, San Francisco, California, USA, Sep. 2011.

[2] T. Okatani and K. Deguchi, "On bias correction for geometric parameter estimation in computer vision," in *Computer Vision and Pattern Recognition, 2009. CVPR 2009. IEEE Conference on*. IEEE, 2009, pp. 959–966.

[3] M. Werman and D. Keren, "A Bayesian method for fitting parametric and nonparametric models to noisy data," *IEEE Transactions on Pattern Analysis and Machine Intelligence*, vol. 23, no. 5, pp. 528–534, 2001.

[4] K. Gilholm and D. Salmond, "Spatial distribution model for tracking extended objects," in *Radar, Sonar and Navigation, IEE Proceedings-*, vol. 152, no. 5. IET, 2005, pp. 364–371.

[5] W. Gander, G. H. Golub, and R. Strebel, "Least-squares fitting of circles and ellipses," *Bulletin of the Belgian Mathematical Society Simon Stevin*, vol. 3, no. 5, pp. 63–84, 1996.

[6] P. Lancaster and K. Salkauskas, "Curve and surface fitting. an introduction," *London: Academic Press, 1986*, vol. 1, 1986.

[7] A. Fitzgibbon, M. Pilu, and R. B. Fisher, "Direct least square fitting of ellipses," *Pattern Analysis and Machine Intelligence, IEEE Transactions on*, vol. 21, no. 5, pp. 476–480, 1999.

[8] F. Faion, A. Zea, M. Baum, and U. D. Hanebeck, "Partial Likelihood for Unbiased Extended Object Tracking," in *Proceedings of the 18th International Conference on Information Fusion (Fusion 2015)*, Washington D. C., USA, Jul. 2015.

[9] D. R. Cox, "Partial likelihood," *Biometrika*, vol. 62, no. 2, pp. 269–276, 1975.

[10] K.-i. Kanatani, "Statistical bias of conic fitting and renormalization," *IEEE Transactions on Pattern Analysis and Machine Intelligence*, vol. 16, no. 3, pp. 320–326, 1994.

[11] F. Faion, A. Zea, and U. D. Hanebeck, "Reducing Bias in Bayesian Shape Estimation," in *Proceedings of the 17th International Conference on Information Fusion (Fusion 2014)*, Salamanca, Spain, Jul. 2014.

[12] F. Faion, M. Dolgov, A. Zea, and U. D. Hanebeck, "Closed-form bias reduction for shape estimation with polygon models," in *Information Fusion (FUSION), 2016 19th International Conference on*. IEEE, 2016, pp. 581–588.